Geophysical Research Letters

RESEARCH LETTER
10.1029/2022GL099013

# Wavefield Migration Imaging of Moho Geometry and Upper Mantle Structure Beneath Southern New England

**Yantao Luo[1], Maureen D. Long[1], Stéphane Rondenay[2], Paul Karabinos[3], and Yvette D. Kuiper[4]**

[1]Department of Earth and Planetary Sciences, Yale University, New Haven, CT, USA, [2]Department of Earth Science, University of Bergen, Bergen, Norway, [3]Geosciences Department, Williams College, Williamstown, MA, USA, [4]Department of Geology and Geological Engineering, Colorado School of Mines, Golden, CO, USA

**Key Points:**

- We conducted 2-D wavefield migration on a dense seismic array across northern Connecticut to investigate crust and upper mantle structures
- We resolved a doubled Moho beneath the Laurentian margin as well as a relict slab and a low-velocity anomaly in the upper mantle
- Migration provides insights unattainable by receiver functions, including the Moho velocity contrast and the geometry of the relict slab

**Supporting Information:**

Supporting Information may be found in the online version of this article.

**Correspondence to:**

Y. Luo,
yantao.luo@yale.edu

**Citation:**

Luo, Y., Long, M. D., Rondenay, S., Karabinos, P., & Kuiper, Y. D. (2022). Wavefield migration imaging of Moho geometry and upper mantle structure beneath southern New England. *Geophysical Research Letters*, *49*, e2022GL099013. https://doi.org/10.1029/2022GL099013

Received 8 APR 2022
Accepted 17 JUN 2022

**Author Contributions:**

**Conceptualization:** Yantao Luo, Maureen D. Long
**Data curation:** Yantao Luo
**Formal analysis:** Yantao Luo, Maureen D. Long, Stéphane Rondenay
**Funding acquisition:** Maureen D. Long
**Investigation:** Yantao Luo, Maureen D. Long, Stéphane Rondenay, Paul Karabinos, Yvette D. Kuiper
**Methodology:** Yantao Luo, Stéphane Rondenay
**Project Administration:** Maureen D. Long
**Resources:** Yantao Luo, Maureen D. Long
**Software:** Yantao Luo, Stéphane Rondenay
**Supervision:** Maureen D. Long



**Abstract** The crust and upper mantle beneath the New England Appalachians exhibit a large offset of the Moho across the boundary between Laurentia and accreted terranes and several dipping discontinuities, which reflect Paleozoic or younger tectonic movements. We apply scattered wavefield migration to the SEISConn array deployed across northern Connecticut and obtain insights not previously available from receiver function studies. We resolve a doubled Moho at a previously imaged Moho offset, which may reflect westward thrusting of rifted Grenville crust. The migration image suggests laterally variable velocity contrasts across the Moho, perhaps reflecting mafic underplating during continental rifting. A west-dipping feature in the lithospheric mantle is further constrained to have a slab-like geometry, representing a relict slab subducted during an Appalachian orogenic event. Localized low seismic velocities in the upper mantle beneath the eastern portion of the array may indicate that the Northern Appalachian Anomaly extends relatively far to the south.

**Plain Language Summary** Tectonic processes in the geologic past, such as the formation and breakup of supercontinents, modified the deep structures of the crust and upper mantle beneath eastern North America. In this study, we use a seismic imaging technique based on scattered wavefield back-projection to investigate deep structures beneath southern New England. This imaging technique, which relies on seismic wave energy from distant earthquakes, is capable of resolving km-scale structures when applied to data from closely spaced seismometers (~10 km station spacing). We image an abrupt, step-like change of the crustal thickness beneath southern New England; the details of this feature suggest a complicated tectonic history during the formation of the Appalachian Mountains. A west-dipping interface in the upper mantle suggests the presence of a relict slab beneath southern New England, associated with a past subduction event. A region of low seismic velocity in the upper mantle beneath southeastern New England may reflect past impingement of a mantle plume or modern upwelling of asthenospheric mantle.

## 1. Introduction

Southern New England exhibits diverse geologic units and paleo-plate boundaries exposed at the surface, resulting from two past supercontinent cycles. Mesoproterozoic Grenville orogenesis created the Grenville orogenic belt and led to the assembly of the supercontinent Rodinia (Rivers, 1997; Tollo et al., 2004). Following the breakup of Rodinia, the margin of the Grenville belt formed the eastern edge of Laurentia (Figure 1a), which was affected by subsequent accretionary and collisional events during Paleozoic Appalachian orogenesis. Appalachian orogenesis involved various subduction events leading to the sequential accretion of several Gondwanan-derived terranes (Hatcher, 2010; Tollo et al., 2010). At the latitude of southern New England, these include the Moretown terrane accreted during the Ordovician Taconic orogeny, all or part of Ganderia accreted during the Silurian Salinic orogeny, and Avalonia accreted during the latest Silurian-Devonian Acadian orogeny (e.g., Hepburn et al., 2021; Kay et al., 2017; Macdonald et al., 2014; Rast et al., 1993). The subsequent Pennsylvanian-Permian Alleghenian orogeny featured the collision of composite Laurentia with Gondwana, leading to the assembly of the supercontinent Pangea, which rifted apart during the Mesozoic (Frizon de Lamotte et al., 2015; Sacks & Secor, 1990). The Mesozoic rifting event opened the Hartford basin in the central part of southern New England (Hubert et al., 1992; Withjack & Schlische, 2005).

These past tectonic events not only shaped the bedrock geologic features exposed at the surface today, but also modified the structure deep in the crust and lithospheric mantle. The lithospheric expression of past tectonic

**Validation:** Yantao Luo
**Visualization:** Yantao Luo
**Writing – original draft:** Yantao Luo
**Writing – review & editing:** Yantao Luo, Maureen D. Long, Stéphane Rondenay, Paul Karabinos, Yvette D. Kuiper

events can be studied using scattered wave imaging methods, including active source seismic refraction/reflection studies (e.g., Cook et al., 1981; Hughes & Luetgert, 1991), teleseismic Ps and Sp receiver functions (e.g., Hopper et al., 2017; Levin et al., 2017), and the scattered wavefield migration technique (e.g., Hopper et al., 2016). Recent continental-scale imaging beneath eastern North America using Ps receiver functions revealed that the Appalachian crust is generally thinner than the Laurentian crust and that there is a step-like change of Moho depth near the eastern edge of exposed Laurentian crust along portions of the margin (Li et al., 2018, 2020). More detailed investigations of Moho geometry across various terrane boundaries, and other small-scale lithospheric features that may reflect past tectonic processes, have recently been carried out in eastern North America using dense broadband seismic arrays (Levin et al., 2017; Long et al., 2019; Luo et al., 2021; Parker, et al., 2013).

A recent Ps receiver function study using data from the Seismic Experiment for Imaging Structure Beneath Connecticut (SEISConn) array confirmed a drastic ∼15 km offset in Moho depth near the surface boundary between Laurentia and accreted terranes, which was not compensated by surface topography, as well as several dipping discontinuities in the crust and lithospheric mantle (Luo et al., 2021). These features likely have important tectonic implications, but the receiver function technique has some significant limitations due to its assumption of a 1-D horizontally layered model, which means that dipping interfaces and diffractions from finer scale features are not resolved properly (Rondenay, 2009). Here, we present new images produced by back-propagating scattered wavefields recorded at SEISConn stations to depth (Bostock et al., 2001). These new images provide additional constraints on the geometry of the Moho and upper mantle structure beneath southern New England. The goal of this study is to use our new scattered wavefield images to build on previous insights based on receiver function analysis and shed new light on the complex tectonic history of the region.

## 2. Data and Methods

The SEISConn array (Figure 1a) consisted of 15 broadband seismometers deployed in northern Connecticut and Rhode Island between 2015 and 2019 (Long & Aragon, 2020). The linear array had an aperture of ∼150 km with ∼11 km station spacing. The array traversed several major tectonic boundaries, including the eastern edge of Laurentia, the borders of the Hartford rift basin, and the western edge of Avalonia (Figure 1a). The dense station spacing of the SEISConn array supports the application of the scattered wavefield migration technique, which is a multichannel inversion method that requires densely sampled data to avoid spatial aliasing (Rondenay et al., 2005).

The imaging workflow extracts scattered wavefields recorded at each station, and backpropagates these wavefields to potential point scatterers in the subsurface by stacking them along diffraction hyperbolae, ultimately resolving the material property perturbations at each point scatterer (P wave velocity $\frac{\delta\alpha}{\alpha}$, S wave velocity $\frac{\delta\beta}{\beta}$, and density $\frac{\delta\rho}{\rho}$) (Bostock et al., 2001; Bostock & Rondenay, 1999). Dependence of scattered wavefields on each material property perturbation varies with scattering modes, and phases that are first reflected at the free surface and then backscattered at the point scatterer (PPp, PPs, PSp, PSsv, PSsh), are included in the migration, in addition to the forward-scattered Ps phase. In practice, for some key modes the density perturbation $\frac{\delta\rho}{\rho}$ has too small an effect to be reliably resolved, and the S-wave velocity perturbation $\frac{\delta\beta}{\beta}$ is typically best resolved and most interpretable (Chen et al., 2013; Mann et al., 2019; Pearce et al., 2012). Additional details of the imaging approach and event selection are discussed in Text S1 and S2 in Supporting Information S1.

## 3. Results

Our migration results for S-wave velocity perturbations using 56 selected events (Figure 1b) are shown in Figure 2. Figure 2a plots the migration using only forward-scattered Ps phase; Figure 2b stacks backscattered phases (PPs, PSp, PSsv, PSsh; migration images for each individual backscattered phase are shown in Figure S1 in Supporting Information S1); Figure 2c combines forward-scattered and backscattered phases to construct a composite migration image; Figure 2d shows the uncertainty in the composite migration image derived from a bootstrap sampling approach, described below. We use a higher frequency cutoff for the forward-scattered Ps phase than for backscattered phases, because the forward-scattered phase has lower spatial resolution than backscattered phases at the same frequency (Bostock, 1999). The migration image displays the perturbations from background reference

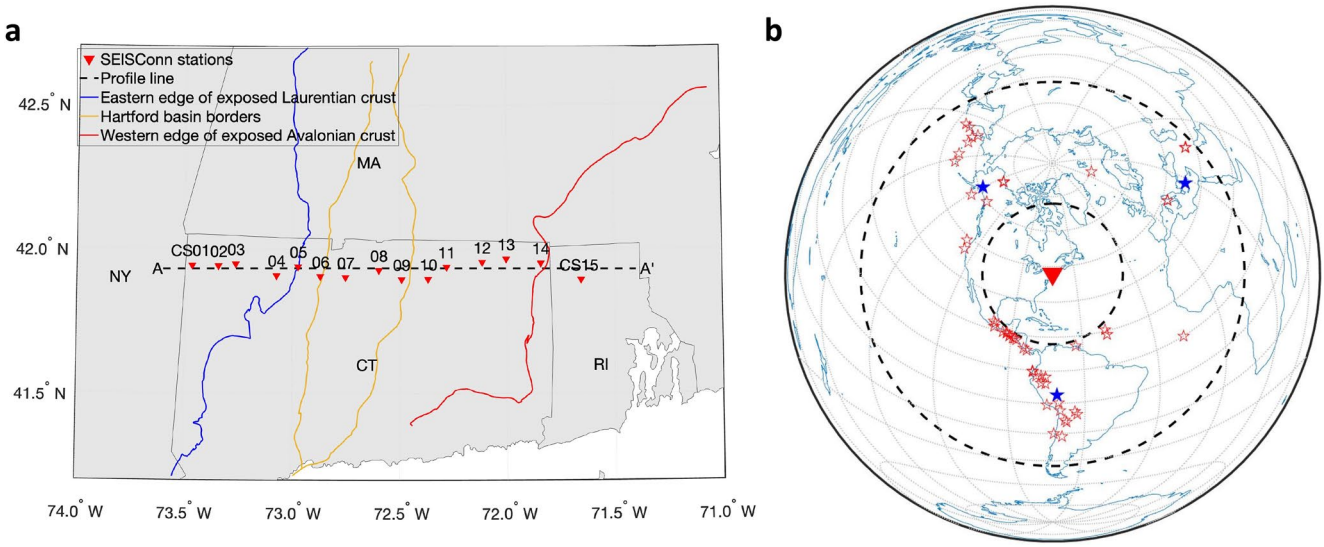


**Figure 1.** Maps of stations (a) and events (b) used in this study. (a) Red triangles denote SEISConn stations. The black dashed line A-A' is the projected profile line. Colored lines show the surface boundaries of the eastern edge of Laurentia (blue), the Mesozoic Hartford rift basin (yellow), and the western edge of Avalonia (red). U.S. state names are shown with abbreviations (CT, Connecticut; MA, Massachusetts; NY, New York; RI, Rhode Island). (b) Red triangle represents the center of the SEISConn array. Red stars denote earthquakes used to construct migration images, within the epicentral distance limits of 30° and 90° (black dashed circles). Blue filled stars mark the three events used to construct Figure S5a in Supporting Information S1.

model at each imaging point. In our plotting scheme, lighter shading on the migration image corresponds to velocities that are faster than the background model, and darker shading corresponds to slower velocities. A rapid increase of seismic velocities with depth, then, will manifest as a drastic change from darker to lighter shading.

Features shown in the migration results align with those resolved in previous receiver function results (Luo et al., 2021), and provide additional detailed information on their geometries. The Moho discontinuity is visible in all migration images as a transition from a dark layer to a light layer beneath; this transition is marked with a yellow dashed line in our annotated images (Figure 3). We observe a relatively deep Moho beneath the western portion of the array (~50 km). To the east, the Moho abruptly shallows from ~50 to ~35 km between stations CS03 and CS04. This Moho depth change appears to be very sharp and step-like, rather than gradual and slope-like. Furthermore, the deeper and shallower Moho appears to overlap, producing a "doubled Moho" geometry in the vicinity of the offset, which was hinted at in previous receiver function images (Luo et al., 2021); a similar Moho geometry has recently been revealed just to the north beneath western Massachusetts (Masis Arce et al., 2022). The migration technique avoids the effect of horizontal averaging in receiver function images, and more convincingly resolves the extent of the shallower and deeper Moho interfaces. Furthermore, this region of the image shows low bootstrap uncertainties (Figure 2d), suggesting that this feature is statistically robust. To the east of the offset, the Moho shallows slightly in the central portion of the array, beneath the Hartford Rift Basin, and then gradually deepens toward the eastern end of the array. We note that a restriction of the migration technique is that it suffers from spatial aliasing at depths shallower than twice the station spacing (Rondenay et al., 2005). Given our ~11 km station spacing, we do not interpret structures within the crust in this study, although previous receiver function imaging (Luo et al., 2021) has shed light on intracrustal structures beneath SEISConn. One other downside of including multiple phases is the leakage of one phase into another, producing ghost artifacts, as illustrated in Figure S2 in Supporting Information S1.

The absolute velocity perturbation amplitudes suggested by the migration images are not exact, because of the poorly resolved density perturbation $\frac{\delta\rho}{\rho}$ and necessary simplifications due to imperfect data coverage (Rondenay et al., 2001; Shragge et al., 2001). However, relative amplitudes in a single migration image are meaningful and interpretable (Hopper et al., 2016). We can therefore estimate the relative magnitude of the velocity contrast across the Moho discontinuity (by calculating the difference between the minimum and maximum S-velocity perturbations above and below the hypothesized Moho) and characterize how it varies along the profile. A plot of estimated shear velocity contrast across the Moho along the array, computed at different frequencies and with errors estimated from bootstrap resampling, is shown in Figure 4. We find that the Moho velocity contrast is

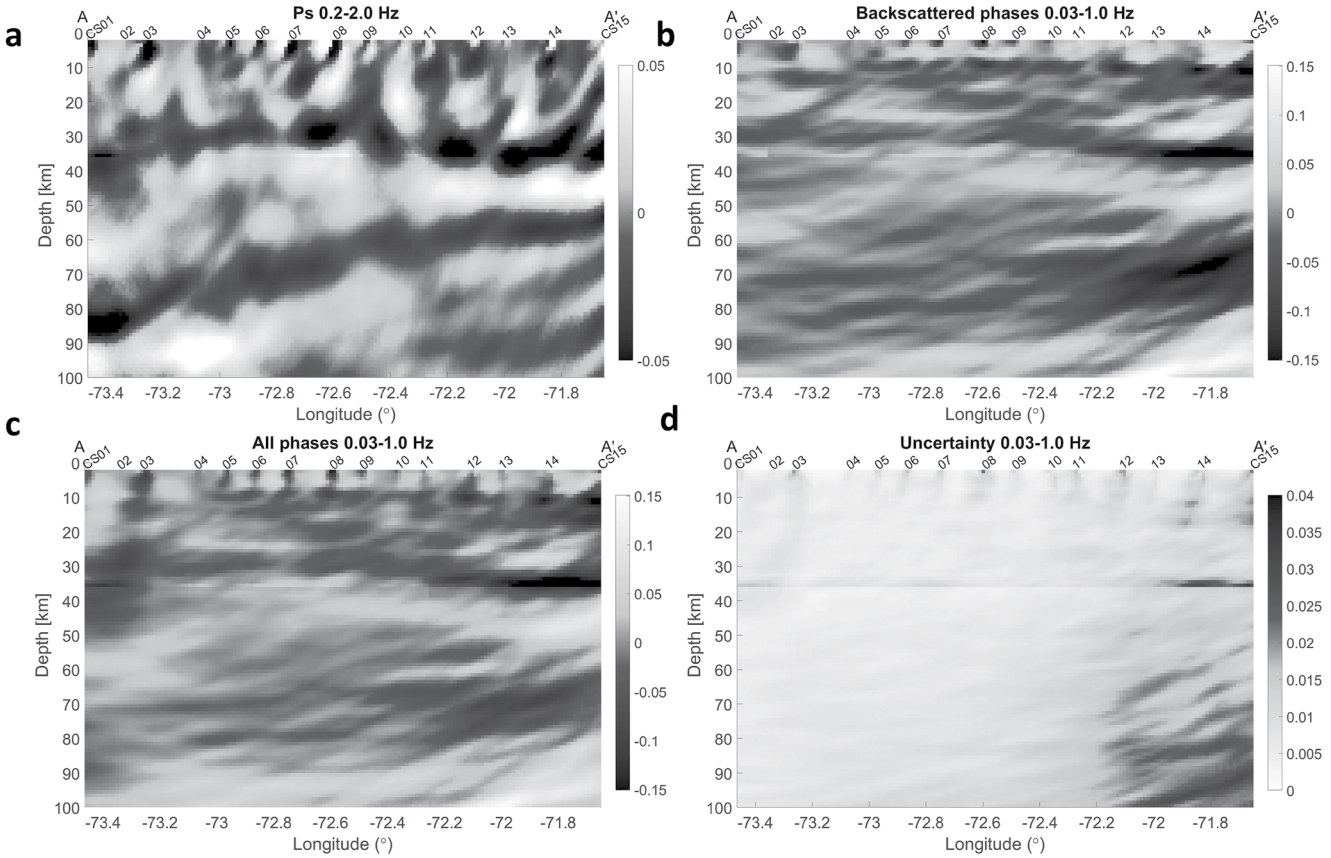


**Figure 2.** Scattered wavefield migration images of S-wave velocity perturbations $\left(\frac{\delta\beta}{\beta}\right)$ constructed using different phases. Lighter regions have positive velocity perturbations and darker regions have negative velocity perturbations. The horizontal line visible in each image at 35 km depth is an artifact from the 1-D background velocity model (see Text S1 in Supporting Information S1). (a) Migration image generated using forward-scattered Ps phase, band-pass filtered between 0.2 and 2.0 Hz. (b) Migration image generated using backscattered phases (PPs, PSp, PSsv, PSsh), band-pass filtered between 0.03 and 1.0 Hz. (c) Composite migration image generated using both forward-scattered and backscattered phases, band-pass filtered between 0.03 and 1.0 Hz. (d) Uncertainty in the composite migration image derived from the bootstrap resampling. Lighter regions have smaller uncertainty and darker regions have larger uncertainty.

larger beneath the eastern portion of the array than beneath the western and central portions. Although the magnitude of velocity contrast variations changes with varying frequency, the observation of larger velocity contrast beneath the eastern portion holds across all frequency bands tested.

In the upper mantle, we observe a continuous west-dipping feature that cuts across the entire profile; a similar feature was identified in the receiver function study and interpreted as a relict slab (Luo et al., 2021). The migration image using forward-scattered Ps phase (Figure 2a) clearly shows the slab-like geometry of this feature. Migration images using backscattered phases (Figures 2b and 2c) likely resolve the top and bottom interfaces of this feature separately. The bottom interface, potentially the Moho of the relict slab, is marked as the blue dashed line in Figure 3 from ~60 km depth near the eastern end of the profile to ~90 km near the western end. The appearance of this feature in PPp phase (Figure S1a in Supporting Information S1) further confirms the robustness of this feature. Beneath this west-dipping feature, we also observe a prominent low-velocity feature, limited in extent to the eastern portion of the array, at 60–80 km depth. This localized low-velocity feature, annotated with the red dashed line in Figure 3b, is hinted at only by backscattered phases, so it may be bounded by relatively smooth velocity gradients instead of sharp velocity contrasts. Interestingly, we observe some dependence on frequency for the identified mantle features. In Ps migration images with varied frequencies (Figure S3 in Supporting Information S1), the west-dipping feature is better resolved at higher frequencies, which is consistent with the presence of a nearby interface with opposite velocity contrast, such that destructive interference hides this feature at lower frequencies. In composite migration images with varied frequencies (Figure S4 in Supporting

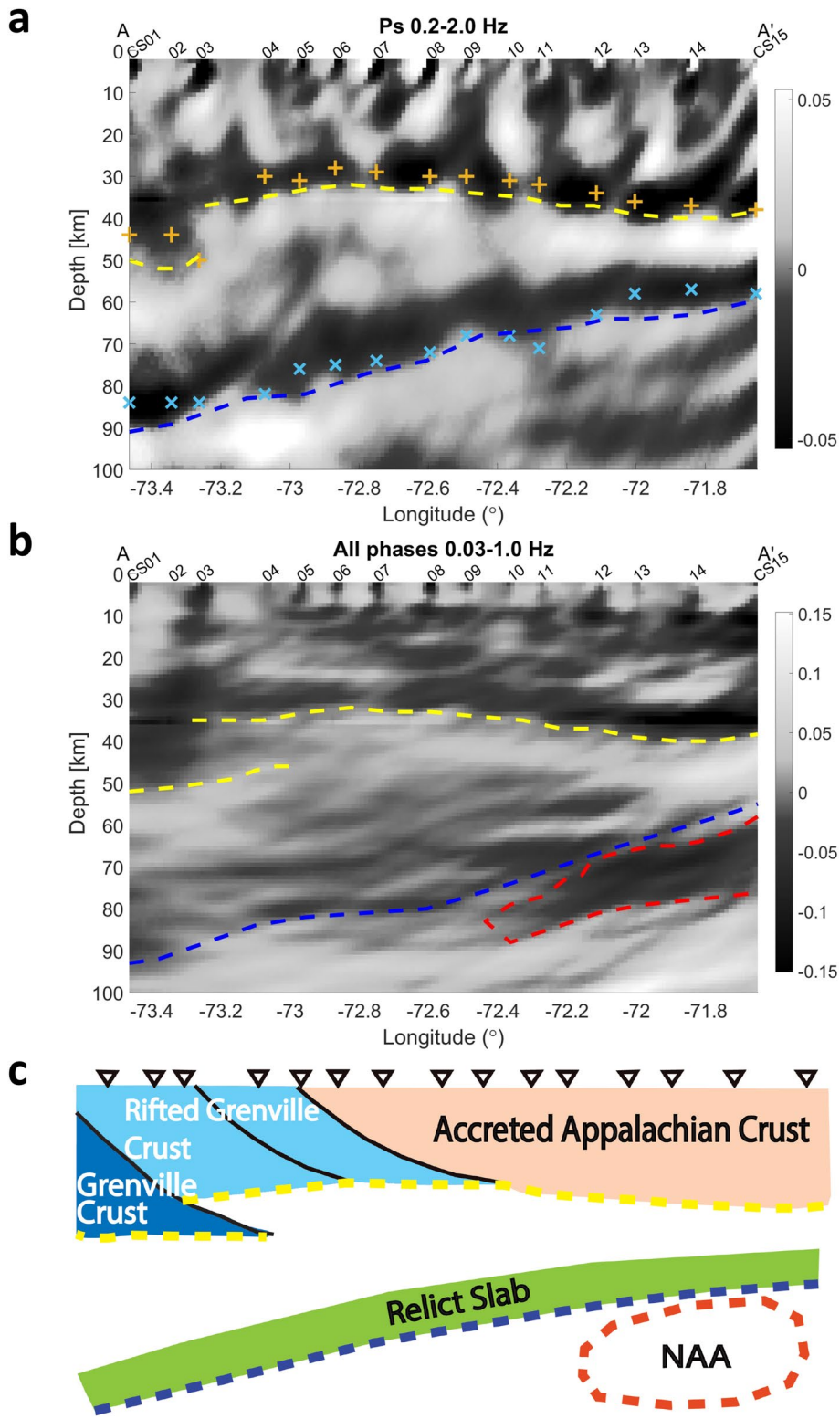


**Figure 3.** (a) Annotated version of Figure 2a, the migration image made with only Ps phase band-passed filtered between 0.2 and 2.0 Hz. Markers denote corresponding features observed in single-station stacked receiver functions band-passed between 0.2 and 2.0 Hz (Luo et al., 2021). (b) Annotated version of Figure 2c, the composite migration image made with all available phases, band-passed filtered between 0.03 and 1.0 Hz. (c) Schematic diagram showing one possible model to explain observed features. Solid black lines are hypothesized crustal boundaries, not constrained by the migration. NAA—Northern Appalachian Anomaly. Plotting conventions for migration results are as in Figure 2. Colored dashed lines highlight the Moho discontinuity (yellow), a west-dipping elongate feature in the mantle lithosphere (blue), and a strong low-velocity anomaly beneath the eastern portion of the array (red).

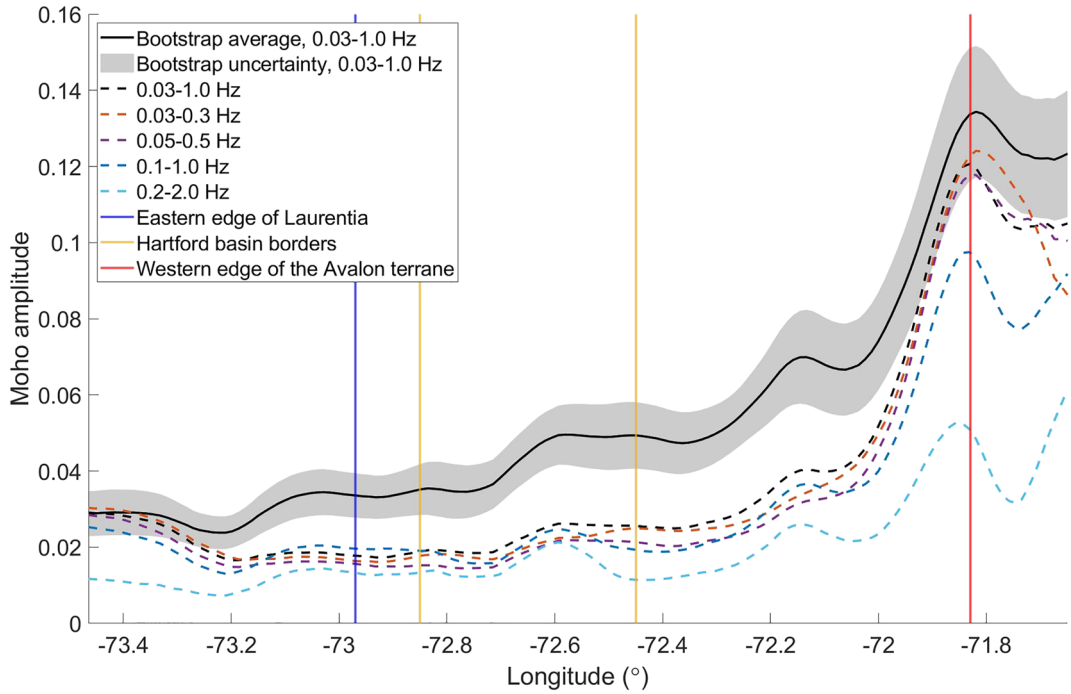


**Figure 4.** Estimates of the relative S-wave velocity contrast (unitless) across the Moho discontinuity. The black solid line and shaded region show the result and uncertainty estimate from bootstrap resampling. Colored dashed lines show results from individual migration images based on the same set of 56 events but with different frequency contents, as shown by the legend.

Information S1), the localized low-velocity anomaly beneath the eastern portion of the array seems to be more prominent at lower frequencies and suppressed at higher frequencies.

To test the robustness of our images and confirm that the features we interpret are not skewed or dominated by a particular collection of events, we generated a suite of migration images with different event combinations. We performed a migration using only three representative events from different backazimuths (Figure 1b); the resulting image (Figure S5a in Supporting Information S1) faithfully recovers the major features identified using the full set of events, though unsurprisingly it has more prominent ripple-like artifacts due to the small amount of data used. We also conducted a bootstrap resampling test to evaluate the stability of the migration results. We randomly resampled the event list and then performed migrations using 1000 such resampled event sets. Each of the three major features identified in the original image are preserved in the bootstrap average images (Figure S5b in Supporting Information S1), so they are likely to be stable features. One caveat gleaned from the bootstrap resampling tests is that although the uncertainty (Figure 2d) is generally low and mostly uniform throughout the model space, it is somewhat higher beneath the eastern portion of the array, near where we observe the localized low-velocity feature. Therefore, we must exercise some caution in interpreting this feature.

## 4. Discussion

### 4.1. Crustal Structure

A crustal thickness difference between Laurentia and the Appalachian accreted terranes has been observed in several large-scale seismic studies in the central and northern Appalachians (e.g., Li et al., 2018; Shen & Ritzwoller, 2016). Distinct Moho offsets or steps have also been suggested in other tectonic settings, such as the Northern US Cordillera (DiCaprio et al., 2020), the Tibetan Plateau (Zhu & Helmberger, 1998), and New Zealand (Salmon et al., 2011), and attributed to various causes. A natural explanation for the observed Moho offset is that it results from the Paleozoic juxtaposition of crustal blocks (Laurentian Grenville crust to the west and Appalachian crust to the east) with preexisting crustal thickness differences. However, Li et al. (2020) showed that the Moho depth transition from Laurentia to Appalachians is considerably sharper beneath southern New England and the central Appalachians than elsewhere along the margin. Indeed, the distinct Moho depth offset resolved

in this study was not found in a similar migration study for the southern Appalachians (Hopper et al., 2016). It is plausible, then, that the Moho offset may have been affected by other factors. For example, Hillenbrand et al. (2021) argued that orogenic collapse at ca. 330 Ma to 300 Ma of their proposed Acadian orogenic plateau resulted in an over-thinned crust in southern New England, which could contribute to the Moho offset. Luo et al. (2021) discussed another potential model for the Moho offset across the edge of Laurentia, which invoked underthrusting of the Laurentian crust to the east beneath accreted terranes.

The composite migration image (Figure 3b) shows that the Moho transition beneath CS03 and CS04 is not just a simple "step," but reflects at least 20 km overlap between deeper and shallower Moho. The surface boundary between Laurentia and accreted Appalachian terranes is located near station CS05 (Figure 1a), but our imaging suggests that the shallower Moho extends ~20 km to the west of this surface boundary. Therefore, the observed offset in Moho depth may plausibly reflect the boundary between two Laurentian Grenville crustal blocks instead of the boundary between Grenville and accreted Appalachian crust. During the Taconic orogeny, the rifted margin of Laurentia was partially subducted beneath the Gondwanan-derived Moretown terrane in an east-dipping subduction zone (Macdonald et al., 2014). The external basement massifs in western New England are composed of Grenville crust overlain by Neoproterozoic rift clastic rocks, which likely formed during the rifting of Rodinia (e.g., Stanley & Ratcliffe, 1985). The Neoproterozoic normal faults may have been reactivated during the Taconic orogeny when the massifs were thrust westward. Therefore, one explanation for the location of the Moho offset and the doubled Moho near the offset is that rifted Grenville crust in the east was thrust over Grenville crust toward the west along preexisting rift faults (Figure 3c). Further crustal shortening during the Acadian orogeny, along with orogenic collapse of the Acadian plateau and crustal thinning proposed by Hillenbrand et al. (2021), may have augmented the sharp nature of the Moho step.

To the east of the Moho offset, the Moho depth varies smoothly, but there is significant variability in the inferred relative shear velocity contrast across with Moho, with a marked increase in Moho velocity contrast near the eastern end of the array (Figure 4). The relatively smaller Moho velocity contrast beneath the western and central portions of the array may imply relatively higher-velocity lower crust. Beneath the western portion of the array, the Laurentian crust of Grenville origin may have been thickened by mafic magmatic underplating during the Proterozoic (Durrheim & Mooney, 1994; Petrescu et al., 2016; Yang & Gao, 2018), yielding a relatively high-velocity lower crust and thus a smaller than typical Moho velocity contrast. Beneath the Hartford Rift Basin in the central portion of the array, a previous ambient noise tomography study (Gao et al., 2020) identified unusually high-velocity lower crust, suggesting that it may have been caused by mafic magmatic underplating associated with the Central Atlantic Magmatic Province event during the breakup of Pangea (McHone, 1996; Withjack et al., 2012). Our finding of a relatively small velocity contrast across the Moho beneath Laurentia and the Hartford Basin supports these interpretations.

### 4.2. Upper Mantle Structure

The slab-like shape of the west-dipping feature in the upper mantle is much better resolved in the Ps migration image (Figure 3a) than in our previous receiver function-based images (Luo et al., 2021). Our new images lend support to our prior interpretation (Luo et al., 2021) that this feature corresponds to a relict slab from a previous subduction episode of which the shallow segment is lodged in the highly viscous lithospheric mantle, while its deeper segment has broken off and sunk into the deeper mantle. This feature is obscured at lower frequencies (Figure S3 in Supporting Information S1), suggesting destructive interference by another nearby interface, which is probably the top of the subducted oceanic crust, hinted at in the composite migration image (Figure 3b). Given the spatial resolution of about half the incident wavelength (Bostock, 1999), the emergence of this feature between the 0.5 Hz cutoff image and the 1.0 Hz cutoff image (Figure S3 in Supporting Information S1) suggests a distance of 4–8 km (assuming $V_p \sim 8$ km/s) between two interfaces, a reasonable thickness for oceanic crust. This feature is shallowly dipping (about 11° dip angle), possibly reflecting a relict slab resulting from nearly flat-slab subduction event during the Acadian orogeny, as previously suggested (Bagherpur Mojaver et al., 2021; Murphy & Keppie, 2005). However, the inferred relict slab projects well east of the Avalon-Ganderia suture zone at the surface, which is located near station CS14 of the SEISConn array (Figure 1a). One possible interpretation is that the shallow part of the Avalon suture was displaced westward during late- or post-Acadian crustal thickening (Hillenbrand & Williams, 2021) or later collisional events. The relict slab may record the Late Devonian "Neoacadian" orogeny, but the nature of this event is unclear at the latitude of southern New England (e.g.,

Kuiper et al., 2017; van Staal et al., 2009). It is also possible that this relict feature resulted from the Alleghenian orogeny, which led to the closure of the Rheic Ocean and the formation of Pangea. However, it is unclear whether the subduction polarity during the Alleghenian closure of the Rheic Ocean was west-dipping (e.g., Domeier & Torsvik, 2014). Despite these uncertainties, our new migration imaging results provide support for a west-dipping remnant slab beneath southern New England, providing valuable information for any future models for the tectonic evolution of this region.

The localized low-velocity feature beneath the eastern portion of the array is less prominent in images made with higher-frequency data (Figure S4 in Supporting Information S1), in contrast to the west-dipping remnant slab feature. We infer, therefore, that this feature likely represents a regional upper mantle velocity anomaly bounded by a relatively smooth velocity gradient, such that high-frequency waves are not scattered at its top boundary. We propose that it may be associated with the Northern Appalachian Anomaly (NAA), a prominent low-velocity anomaly centered beneath central New England that has been imaged in previous seismic tomography studies (e.g., Levin et al., 1995; Porter et al., 2016). The NAA has been interpreted as a relict feature from the passage of the Great Meter hotspot roughly 110 Ma (Eaton & Frederiksen, 2007; Li et al., 2003), as a modern feature that reflects ongoing asthenospheric upwelling (Levin et al., 2018; Menke et al., 2016), or a combination of both (Tao et al., 2020). The localized low-velocity region resolved in our migration images suggests that the NAA may extend as far south as northern Connecticut and Rhode Island beneath the eastern end of the SEISConn array. This hypothesis is also supported by the small SKS splitting delay times observed at eastern SEISConn stations (Lopes et al., 2020), which may reflect asthenospheric upwelling associated with the NAA.

## 5. Summary and Outlook

The scattered wavefield migration technique applied to SEISConn data images a doubled Moho near the edge of Laurentia that may have resulted from thrusting of rifted Grenville crust during the Taconic and/or Acadian orogenies. The clearly imaged west-dipping feature in the mantle provides additional support to the hypothesis that a Paleozoic subduction event resulted in a relict slab beneath southern New England. Our results suggest that the NAA in the upper mantle may extend as far south as northern Connecticut. We have shown that scattered wavefield migration imaging can provide an excellent complement to receiver function imaging for dense array data sets. Ongoing work on imaging lithospheric structure beneath southern New England, including its seismic anisotropy, using a suite of methods with different strengths and limitations, is providing a comprehensive picture of the structure and evolution of this tectonically complex region.

## Data Availability Statement

Data used in this study (https://doi.org/10.7914/SN/XP_2015) are archived at the Incorporated Research Institutions for Seismology (IRIS) Data Management Center (DMC) and are publicly available at http://service.iris.edu/fdsnws/dataselect/1/.

**Acknowledgments**
Collection and analysis of SEISConn data were funded by Yale University and by the National Science Foundation via grants EAR-1150722 and EAR-1800923. The authors thank the station hosts and field personnel who made the SEISConn experiment possible, particularly participants in the Field Experiences for Science Teachers (FEST) program (Long, 2017). The authors are grateful to collaborators and colleagues on various aspects of SEISConn data analysis and interpretations. We thank Mike Williams and Derek Schutt for constructive comments that helped to improve the paper.

## References

Bagherpur Mojaver, O., Darbyshire, F., & Dave, R. (2021). Lithospheric structure and flat-slab subduction in the northern Appalachians: Evidence from Rayleigh wave tomography. *Journal of Geophysical Research: Solid Earth*, *126*(4), e2020JB020924. https://doi.org/10.1029/2020JB020924

Bostock, M. G. (1999). Seismic waves converted from velocity gradient anomalies in the Earth's upper mantle. *Geophysical Journal International*, *138*(3), 747–756. https://doi.org/10.1046/j.1365-246x.1999.00902.x

Bostock, M. G., & Rondenay, S. (1999). Migration of scattered teleseismic body waves. *Geophysical Journal International*, *137*(3), 732–746. https://doi.org/10.1046/j.1365-246x.1999.00813.x

Bostock, M. G., Rondenay, S., & Shragge, J. (2001). Multiparameter two-dimensional inversion of scattered teleseismic body waves 1. Theory for oblique incidence. *Journal of Geophysical Research*, *106*(B12), 30771–30782. https://doi.org/10.1029/2001JB000330

Chen, C.-W., James, D. E., Fouch, M. J., & Wagner, L. S. (2013). Lithospheric structure beneath the High Lava Plains, Oregon, imaged by scattered teleseismic waves. *Geochemistry, Geophysics, Geosystems*, *14*(11), 4835–4848. https://doi.org/10.1002/ggge.20284

Cook, F. A., Brown, L. D., Kaufman, S., Oliver, J. E., & Petersen, T. A. (1981). COCORP seismic profiling of the Appalachian orogen beneath the Coastal Plain of Georgia. *GSA Bulletin*, *92*(10), 738–748. https://doi.org/10.1130/0016-7606(1981)92<738:Cspota>2.0.Co;2

Di Caprio, L., Maiti, T., Dettmer, J., & Eaton, D. W. (2020). Moho structure across the backarc-craton transition in the northern U.S. Cordillera. *Tectonics*, *39*(2), e2019TC005489. https://doi.org/10.1029/2019TC005489

Domeier, M., & Torsvik, T. H. (2014). Plate tectonics in the late Paleozoic. *Geoscience Frontiers*, *5*(3), 303–350. https://doi.org/10.1016/j.gsf.2014.01.002

Durrheim, R. J., & Mooney, W. D. (1994). Evolution of the Precambrian lithosphere: Seismological and geochemical constraints. *Journal of Geophysical Research*, *99*(B8), 15359–15374. https://doi.org/10.1029/94JB00138

Eaton, D. W., & Frederiksen, A. (2007). Seismic evidence for convection-driven motion of the North American plate. *Nature*, *446*(7134), 428–431. https://doi.org/10.1038/nature05675

Frizon de Lamotte, D., Fourdan, B., Leleu, S., Leparmentier, F., & de Clarens, P. (2015). Style of rifting and the stages of Pangea breakup. *Tectonics*, *34*(5), 1009–1029.

Gao, H., Yang, X., Long, M. D., & Aragon, J. C. (2020). Seismic evidence for crustal modification beneath the Hartford rift basin in the northeastern United States. *Geophysical Research Letters*, *47*(17), e2020GL089316. https://doi.org/10.1029/2020gl089316

Hatcher, R. D. (2010). *The Appalachian orogen: A brief summary. From Rodinia to Pangea: The lithotectonic record of the Appalachian region* (Vol. 206, pp. 1–19). Geological Society of America Memoir.

Hepburn, J. C., Kuiper, Y. D., McClary, K. J., Loan, M. L., Tubrett, M., & Buchwaldt, R. (2021). Detrital zircon ages and the origins of the Nashoba terrane and Merrimack belt in southeastern New England, USA. *Atlantic Geology: Journal of the Atlantic Geoscience Society/Atlantic Geology: revue de la Société Géoscientifique de l'Atlantique*, *57*, 343–396. https://doi.org/10.4138/atlgeol.2021.016

Hillenbrand, I. W., & Williams, M. L. (2021). Paleozoic evolution of crustal thickness and elevation in the northern Appalachian orogen, USA. *Geology*, *49*(8), 946–951. https://doi.org/10.1130/g48705.1

Hillenbrand, I. W., Williams, M. L., Li, C., & Gao, H. (2021). Rise and fall of the Acadian altiplano: Evidence for a paleozoic orogenic plateau in New England. *Earth and Planetary Science Letters*, *560*, 116797. https://doi.org/10.1016/j.epsl.2021.116797

Hopper, E., Fischer, K., Rondenay, S., Hawman, R., & Wagner, L. (2016). Imaging crustal structure beneath the southern Appalachians with wavefield migration. *Geophysical Research Letters*, *43*(23), 12054–12062.

Hopper, E., Fischer, K. M., Wagner, L. S., & Hawman, R. B. (2017). Reconstructing the end of the Appalachian orogeny. *Geology*, *45*(1), 15–18. https://doi.org/10.1130/g38453.1

Hubert, J. F., Feshbach-Meriney, P. E., & Smith, M. A. (1992). The Triassic-Jurassic Hartford rift basin, Connecticut and Massachusetts: Evolution, sandstone diagenesis, and hydrocarbon History. *AAPG Bulletin*, *76*(11), 1710–1734. https://doi.org/10.1306/bdff8ab0-1718-11d7-8645000102c1865d

Hughes, S., & Luetgert, J. H. (1991). Crustal structure of the Western new England Appalachians and the Adirondack Mountains. *Journal of Geophysical Research*, *96*(B10), 16471–16494. https://doi.org/10.1029/91JB01657

Kay, A., Hepburn, J. C., Kuiper, Y. D., & Baxter, E. F. (2017). Geochemical evidence for a Ganderian arc/back-arc remnant in the Nashoba Terrane, SE New England, USA. *American Journal of Science*, *317*(4), 413–448. https://doi.org/10.2475/04.2017.01

Kuiper, Y. D., Thompson, M. D., Barr, S. M., White, C. E., Hepburn, J. C., & Crowley, J. L. (2017). Detrital zircon evidence for Paleoproterozoic West African crust along the eastern North American continental margin, Georges Bank, offshore Massachusetts, USA. *Geology*, *45*(9), 811–814. https://doi.org/10.1130/g39203.1

Levin, V., Lerner-Lam, A., & Menke, W. (1995). Anomalous mantle structure at the Proterozoic-Paleozoic boundary in northeastern US. *Geophysical Research Letters*, *22*(2), 121–124. https://doi.org/10.1029/94GL02693

Levin, V., Long, M. D., Skryzalin, P., Li, Y., & López, I. (2018). Seismic evidence for a recently formed mantle upwelling beneath New England. *Geology*, *46*(1), 87–90. https://doi.org/10.1130/g39641.1

Levin, V., Servali, A., VanTongeren, J., Menke, W., & Darbyshire, F. (2017). Crust-mantle boundary in eastern North America, from the (oldest) craton to the (youngest) rift. In *The crust-mantle and lithosphere-asthenosphere boundaries: Insights from xenoliths, orogenic deep sections, and geophysical studies* (Vol. 526). Geological Society of America. https://doi.org/10.1130/2017.2526(06

Li, A., Forsyth, D. W., & Fischer, K. M. (2003). Shear velocity structure and azimuthal anisotropy beneath eastern North America from Rayleigh wave inversion. *Journal of Geophysical Research*, *108*(B8). https://doi.org/10.1029/2002JB002259

Li, C., Gao, H., & Williams, M. L. (2020). Seismic characteristics of the eastern North American crust with Ps converted waves: Terrane accretion and modification of continental crust. *Journal of Geophysical Research: Solid Earth*, *125*(5), e2019JB018727. https://doi.org/10.1029/2019JB018727

Li, C., Gao, H., Williams, M. L., & Levin, V. (2018). Crustal thickness variation in the northern Appalachian Mountains: Implications for the geometry of 3-D tectonic boundaries within the crust. *Geophysical Research Letters*, *45*(12), 6061–6070. https://doi.org/10.1029/2018GL078777

Long, M. D. (2017). The field Experiences for science Teachers (FEST) program: Involving Connecticut high school science Teachers in field Seismology. *Seismological Research Letters*, *88*(2A), 421–429. https://doi.org/10.1785/0220160162

Long, M. D., & Aragon, J. C. (2020). Probing the structure of the crust and mantle lithosphere beneath the southern new England Appalachians via the SEISConn deployment. *Seismological Research Letters*, *91*(5), 2976–2986. https://doi.org/10.1785/0220200163

Long, M. D., Benoit, M. H., Aragon, J. C., & King, S. D. (2019). Seismic imaging of mid-crustal structure beneath central and eastern North America: Possibly the elusive Grenville deformation? *Geology*, *47*(4), 371–374. https://doi.org/10.1130/g46077.1

Lopes, E., Long, M. D., Karabinos, P., & Aragon, J. C. (2020). SKS splitting and upper mantle anisotropy beneath the southern new England Appalachians: Constraints from the dense SEISConn array. *Geochemistry, Geophysics, Geosystems*, *21*(12), e2020GC009401. https://doi.org/10.1029/2020GC009401

Luo, Y., Long, M. D., Karabinos, P., Kuiper, Y. D., Rondenay, S., Aragon, J. C., et al. (2021). High-resolution Ps receiver function imaging of the crust and mantle lithosphere beneath southern new England and tectonic implications. *Journal of Geophysical Research: Solid Earth*, *126*(7), e2021JB022170. https://doi.org/10.1029/2021JB022170

Macdonald, F. A., Ryan-Davis, J., Coish, R. A., Crowley, J. L., & Karabinos, P. (2014). A newly identified Gondwanan Terrane in the northern Appalachian Mountains: Implications for the Taconic orogeny and closure of the Iapetus ocean. *Geology*, *42*(6), 539–542. https://doi.org/10.1130/g35659.1

Mann, M. E., Abers, G. A., Crosbie, K., Creager, K., Ulberg, C., Moran, S., & Rondenay, S. (2019). Imaging subduction beneath mount St. Helens: Implications for slab dehydration and magma transport. *Geophysical Research Letters*, *46*(6), 3163–3171. https://doi.org/10.1029/2018GL081471

Masis Arce, R., Luo, Y., Espinel, K., Yiran, L., Levin, V., Long, M., & Karabinos, P. (2022). A closer look at the offset in crustal thickness beneath northwestern Massachusetts GSA northeastern section–57th annual meeting–2022.

McHone, J. G. (1996). Broad-terrane Jurassic flood basalts across northeastern North America. *Geology*, *24*(4), 319–322. https://doi.org/10.1130/0091-7613(1996)024<0319:Btjfba>2.3.Co;2

Menke, W., Skryzalin, P., Levin, V., Harper, T., Darbyshire, F., & Dong, T. (2016). The northern Appalachian anomaly: A modern Asthenospheric upwelling. *Geophysical Research Letters*, *43*(19), 10173–10179. https://doi.org/10.1002/2016GL070918

Murphy, J. B., & Keppie, J. D. (2005). The Acadian orogeny in the northern Appalachians. *International Geology Review*, *47*(7), 663–687. https://doi.org/10.2747/0020-6814.47.7.663

Parker, E. H., Hawman, R. B., Fischer, K. M., & Wagner, L. S. (2013). Crustal evolution across the southern Appalachians: Initial results from the SESAME broadband array. *Geophysical Research Letters*, *40*(15), 3853–3857. https://doi.org/10.1002/grl.50761

Pearce, F. D., Rondenay, S., Sachpazi, M., Charalampakis, M., & Royden, L. H. (2012). Seismic investigation of the transition from continental to oceanic subduction along the Western Hellenic Subduction Zone. *Journal of Geophysical Research*, *117*(B7). https://doi.org/10.1029/2011JB009023

Petrescu, L., Bastow, I. D., Darbyshire, F. A., Gilligan, A., Bodin, T., Menke, W., & Levin, V. (2016). Three billion years of crustal evolution in eastern Canada: Constraints from receiver functions. *Journal of Geophysical Research: Solid Earth*, *121*(2), 788–811. https://doi.org/10.1002/2015JB012348

Porter, R., Liu, Y., & Holt, W. E. (2016). Lithospheric records of orogeny within the continental US. *Geophysical Research Letters*, *43*(1), 144–153. https://doi.org/10.1002/2015GL066950

Rast, N., Skehan, J. W., Roy, D. C., & Skehan, J. W. (1993). Mid-paleozoic orogenesis in the North Atlantic: The Acadian orogeny. In *The Acadian orogeny: Recent studies in new England, maritime Canada, and the autochthonous foreland* (Vol. 275). Geological Society of America. https://doi.org/10.1130/SPE275-p1

Rivers, T. (1997). Lithotectonic elements of the Grenville Province: Review and tectonic implications. *Precambrian Research*, *86*(3), 117–154. https://doi.org/10.1016/S0301-9268(97)00038-7

Rondenay, S. (2009). Upper mantle imaging with array recordings of converted and scattered teleseismic waves. *Surveys in Geophysics*, *30*(4–5), 377–405.

Rondenay, S., Bostock, M. G., & Fischer, K. M. (2005). Multichannel inversion of scattered teleseismic body waves: Practical considerations and applicability. *Geophysical Monograph-American Geophysical Union*, *157*, 187.

Rondenay, S., Bostock, M. G., & Shragge, J. (2001). Multiparameter two-dimensional inversion of scattered teleseismic body waves 3. Application to the Cascadia 1993 data set. *Journal of Geophysical Research*, *106*(B12), 30795–30807. https://doi.org/10.1029/2000JB000039

Sacks, P. E., & Secor, D. T. (1990). Kinematics of late Paleozoic continental collision between Laurentia and Gondwana. *Science*, *250*(4988), 1702–1705. https://doi.org/10.1126/science.250.4988.1702

Salmon, M. L., Stern, T. A., & Savage, M. K. (2011). A major step in the continental Moho and its geodynamic consequences: The Taranaki–Ruapehu line, New Zealand. *Geophysical Journal International*, *186*(1), 32–44. https://doi.org/10.1111/j.1365-246X.2011.05035.x

Shen, W., & Ritzwoller, M. H. (2016). Crustal and uppermost mantle structure beneath the United States. *Journal of Geophysical Research: Solid Earth*, *121*(6), 4306–4342. https://doi.org/10.1002/2016JB012887

Shragge, J., Bostock, M. G., & Rondenay, S. (2001). Multiparameter two-dimensional inversion of scattered teleseismic body waves 2. Numerical examples. *Journal of Geophysical Research*, *106*(B12), 30783–30793. https://doi.org/10.1029/2001JB000326

Stanley, R. S., & Ratcliffe, N. M. (1985). Tectonic synthesis of the Taconian orogeny in Western new England. *GSA Bulletin*, *96*(10), 1227–1250. https://doi.org/10.1130/0016-7606(1985)96<1227:Tsotto>2.0.Co;2

Tao, Z., Li, A., & Fischer, K. M. (2020). Hotspot signatures at the North American passive margin. *Geology*(5), 525–530. https://doi.org/10.1130/g47994.1

Tollo, R. P., Bartholomew, M. J., Hibbard, J. P., & Karabinos, P. M. (2010). *From Rodinia to Pangea: The lithotectonic record of the Appalachian region*. Geological Society of America. https://doi.org/10.1130/mem206

Tollo, R. P., McLelland, J., Corriveau, L., & Bartholomew, M. J. (2004). *Proterozoic tectonic evolution of the Grenville orogen in north America*. Geological Society of America. https://doi.org/10.1130/mem197

van Staal, C. R., Whalen, J. B., Valverde-Vaquero, P., Zagorevski, A., & Rogers, N. (2009). Pre-Carboniferous, episodic accretion-related, orogenesis along the Laurentian margin of the northern Appalachians. *Geological Society, London, Special Publications*, *327*(1), 271–316. https://doi.org/10.1144/sp327.13

Withjack, M. O., & Schlische, R. W. (2005). A review of tectonic events on the passive margin of eastern North America. *Petroleum Systems of Divergent Continental Margin Basins: 25th Bob S. Perkins Research Conference, Gulf Coast Section of SEPM*.

Withjack, M. O., Schlische, R. W., & Olsen, P. E. (2012). Development of the passive margin of eastern North America: Mesozoic rifting, igneous activity, and breakup. *Regional Geology and Tectonics: Phanerozoic Rift Systems and Sedimentary Basins*, *1*, 301.

Yang, X., & Gao, H. (2018). Full-wave seismic tomography in the northeastern United States: New insights into the uplift mechanism of the Adirondack Mountains. *Geophysical Research Letters*, *45*(12), 5992–6000. https://doi.org/10.1029/2018GL078438

Zhu, L., & Helmberger, D. V. (1998). Moho offset across the northern margin of the Tibetan plateau. *Science*, *281*(5380), 1170–1172. https://doi.org/10.1126/science.281.5380.1170

## References From the Supporting Information

Beylkin, G. (1985). Imaging of discontinuities in the inverse scattering problem by inversion of a causal generalized Radon transform. *Journal of Mathematical Physics*, *26*(1), 99–108. https://doi.org/10.1063/1.526755

Kennett, B. L. N. (1991). The Removal of Free Surface Interactions from Three-Component Seismograms. *Geophysical Journal International*, *104*(1), 153–154. https://doi.org/10.1111/j.1365-246X.1991.tb02501.x

Ulrych, T. J., Sacchi, M. D., & Freire, S. L. M. (1999). Eigenimage processing of seismic sections. In R. L. Kirlin & W. J. Done (Eds.), *Covariance analysis for Seismic Signal Processing* (Vol. 8). Society of Exploration Geophysicists. https://doi.org/10.1190/1.9781560802037.ch12

Van Decar, J. C., & Crosson, R. S. (1990). Determination of teleseismic relative phase arrival times using multi-channel cross-correlation and least squares. *Bulletin of the Seismological Society of America*, *80*(1), 150–169. https://doi.org/10.1785/bssa0800010150